scientific reports

Check for updates

OPEN

Unveiling the anti-inflammatory mechanism of exogenous hydrogen sulfide in Kawasaki disease based on network pharmacology and experimental validation

Ling Yu[1], Qianwen Luo[2], Xiaohui Rao[3], Xiao Xiao[2] & Pinghan Wang[2]✉

Kawasaki disease (KD) is a severe pediatric vasculitis leading to coronary artery complications. Hydrogen sulfide (H_2S), a recognized endogenous gasotransmitter with anti-inflammatory properties, offers potential as a novel treatment for KD through its cardiovascular benefits. However, the specific effects and underlying mechanisms remain unclear. The objective of present study is to investigate the anti-inflammatory and therapeutic effects of exogenous H_2S in KD using network pharmacology and experimental validation. By online database searches, a total of 405 pharmacological targets for H_2S, 826 KD-related targets, and 107 potential therapeutic targets of H_2S for KD were identified. Through PPI analysis and Cytoscape screening, 9 hub genes were filtered, namely TNF, IL6, JUN, AKT1, IL1B, TP53, NFKB1, MAPK1, and RELA. KEGG pathway enrichment indicated that the TLR4/MyD88/NF-κB signaling pathway may play a crucial role in the therapeutic effects of H_2S on KD. Additionally, in vivo experiments confirmed that the treatment of sodium hydrosulfide (NaHS), an H_2S donor, markedly improved body weight, reduced inflammatory pathology in the coronary arteries, and downregulated levels of inflammatory cytokines TNF-α, IL-1β, and IL-6. Furthermore, WB analysis confirmed that NaHS inhibited the expression of TLR4, MyD88, NF-κB, and p-NF-κB. In brief, it is the first to reveal that exogenous H_2S attenuates the inflammatory response in KD via the TLR4/MyD88/NF-κB pathway, highlighting its potential as a novel therapeutic approach for KD. These findings lay a foundation for further development of H_2S-based therapies for KD management.

Keywords Kawasaki disease, Hydrogen sulfide, Network pharmacology, Inflammation, TLR4/MyD88/NF-κB pathway

Kawasaki disease (KD), also referred to mucocutaneous lymph node syndrome, is an acute, self-limited vasculitis predominantly affecting children under five years of age[1,2]. First identified by Dr. Tomisaku Kawasaki in 1967, KD has emerged as the leading cause of acquired heart disease among children in developed countries[3]. The disease is characterized by prolonged fever, mucocutaneous inflammation, lymphadenopathy, and, most critically, coronary artery abnormalities, which can lead to aneurysms and long-term cardiovascular complications[4]. Despite significant research efforts, the precise etiology of KD remains unclear, presenting challenges for the development of targeted therapies. The standard treatment for KD involves high-dose intravenous immunoglobulin (IVIG) combined with aspirin, which has been shown to reduce the incidence of coronary artery aneurysms[5,6]. However, approximately 10–20% of patients are resistant to IVIG therapy, increasing their risk of developing cardiac complications[7]. Additionally, prolonged use of high-dose aspirin is associated with

[1]Key Laboratory of Reproductive Medicine, Center of Reproductive Medicine, Sichuan Provincial Women's and Children's Hospital/The Affiliated Women's and Children's Hospital of Chengdu Medical College, Chengdu Medical College, Chengdu 610045, China. [2]Laboratory Medicine Center, Sichuan Provincial Women's and Children's Hospital/The Affiliated Women's and Children's Hospital of Chengdu Medical College, Chengdu Medical College, Chengdu 610032, China. [3]Department of Clinical Research, Sichuan Clinical Research Center for Cancer, Sichuan Cancer Hospital & Institute, Sichuan Cancer Center, Affiliated Cancer Hospital of University of Electronic Science and Technology of China, Chengdu 610042, China. ✉email: zxcvbnm_345@126.com

adverse effects such as gastrointestinal bleeding and Reye's syndrome[8,9]. These limitations underscore the need for alternative therapeutic strategies that are both effective and have fewer side effects.

Hydrogen sulfide (H_2S) is a colorless, acidic gas known for its characteristic rotten egg odor. Due to its toxicity at concentrations above physiological levels, H_2S has long been regarded as a hazardous compound capable of causing damage to multiple organs[10]. In recent years, H_2S is recognized as the third major endogenous gasotransmitter in biological systems, following carbon monoxide and nitric oxide, which plays a vital role in numerous physiological processes, including vasodilation, anti-inflammation, and cytoprotection[11]. In the cardiovascular system, H_2S modulates vascular tone, inhibits smooth muscle cell proliferation, and reduces oxidative stress[12]. Sodium hydrosulfide (NaHS) is a commonly used H_2S donor that rapidly releases H_2S in biological systems, making it a valuable tool for investigating the therapeutic potential of H_2S[13]. Emerging evidence suggests that H_2S donors like NaHS may offer protective effects in cardiovascular diseases by mitigating inflammation and endothelial dysfunction, processes that are central to the pathogenesis of KD[14–16].

Network pharmacology offers a holistic approach to drug discovery by considering the complex interactions between drugs, targets, and disease networks[17]. This methodology is particularly useful in multifactorial diseases like KD, where multiple signaling pathways are implicated. By integrating systems biology with computational analysis, network pharmacology can identify potential therapeutic targets and elucidate the mechanisms of action of bioactive compounds[18]. Furthermore, it facilitates the understanding of polypharmacology—the ability of drugs to affect multiple targets simultaneously—thereby enabling the identification of synergistic drug combinations that may enhance therapeutic efficacy and reduce adverse effects. Advanced bioinformatics tools and large-scale biological databases are employed to construct and analyze intricate molecular interaction networks, allowing researchers to pinpoint key nodes and pathways that are critical for disease progression and therapeutic intervention[18]. Together, these methodologies enable a comprehensive exploration of drug mechanisms, promoting the discovery of novel therapeutics with enhanced precision and reduced likelihood of resistance. This integrative framework not only advances our understanding of complex disease biology but also streamlines the drug development process, making it more efficient and targeted.

In the present study, we aimed to investigate the pharmacological mechanisms of exogenous H_2S in the context of KD through an integrated approach combining network pharmacology and experimental validation. We constructed a comprehensive network of H_2S-associated targets and KD-related genes to identify key signaling pathways and molecular interactions. Experimental validation was conducted to confirm the computational predictions and assess the therapeutic potential of exogenous H_2S in a KD mouse model. The findings of this study provide a solid foundation for the potential application of exogenous H_2S as a novel therapeutic agent for KD, and offer valuable insights for the development of other safe and effective anti-KD therapies. The detailed workflow of this study is shown in Fig. 1.

Materials and methods

Target prediction and screening of H_2S

First, the 2D.sdf file of H_2S was retrieved from the PubChem database (http://pubchem.ncbi.nlm.nih.gov/) by searching for "CAS 7783-06-4" and then uploaded to the ChEMBL database (https://www.ebi.ac.uk/chembl/)[19] to obtain the canonical SMILES number[20]. The SMILES or H_2S was subsequently utilized in the TargetNet (http://targetnet.scbdd.com/)[21] and STITCH (http://stitch.embl.de/)[22] databases to predict pharmacological targets, specifying "Homo sapiens" as the organism of interest and selecting targets with a probability of ≥ 0.7 and medium confidence scores > 0.4. Furthermore, by querying "CAS 7783-06-4" in the PubChem database[23], the targets validated through experimental studies involving H_2S were obtained from the following entries: "Chemical-Gene Co-Occurrences in Literature", "BioAssay Results", "Chemical-Target Interactions", and "Protein Bound 3D Structures". Utilizing the UniProt database (https://www.uniprot.org/), the identified targets were standardized with "Homo sapiens" as the organism constraint. The targets obtained from the three databases were merged and duplicates were removed to gather the H_2S-related targets.

Identification of KD-related targets

Using the keywords "Kawasaki disease" and "kucocutaneous lymph node syndrome", the KD-related targets was sought across multiple public disease databases, including GeneCards (version 5.18, https://www.genecards.org/)[24], DisGeNET (version 7.0, https://www.disgenet.org/)[25], OMIM (https://omim.org/)[26], and DrugBank (version 5.1.10, https://go.drugbank.com/)[27]. We calibrated the collected disease targets by the UniProt database, with the species parameter restricted to "Homo sapiens". Then, we integrated the results and eliminated redundant values to obtain the final targets associated with KD. Specific criteria for target selection were as follows: targets from GeneCards with a Relevance score greater $\geq$ the average, targets from DisGeNET with a Score_gda ≥ 0.1, and targets from DrugBank categorized as "target" in the TYPE field. Additionally, we uploaded the H_2S-related targets and disease targets to the online tool jVenn (http://bioinfo.genotoul.fr/jvenn/)[28] to identify overlapping targets and generate a Venny diagram. The intersecting targets were recognized as therapeutic targets for NaHS against KD.

Construction of protein-protein interaction (PPI) network and core target screening

To construct PPI network for analyzing interactions between proteins, the shared targets from NaHS-treated KD were uploaded to the STRING database (Version 12.0, https://cn.string-db.org)[29], with the species set as "Homo sapiens" and the minimum interaction score set to "highest confidence (> 0.9)". Subsequently, the PPI network image and the TSV file were downloaded. The latter was then imported into Cytoscape software (Version 3.10.1), where the CytoHubba plugin was employed to perform core target identification using 12 different topological analysis methods. The top 10 ranked targets from each of the 12 algorithms were compiled to identify the key targets[30]. The total number of times each target appeared across the algorithms was calculated and ranked, and

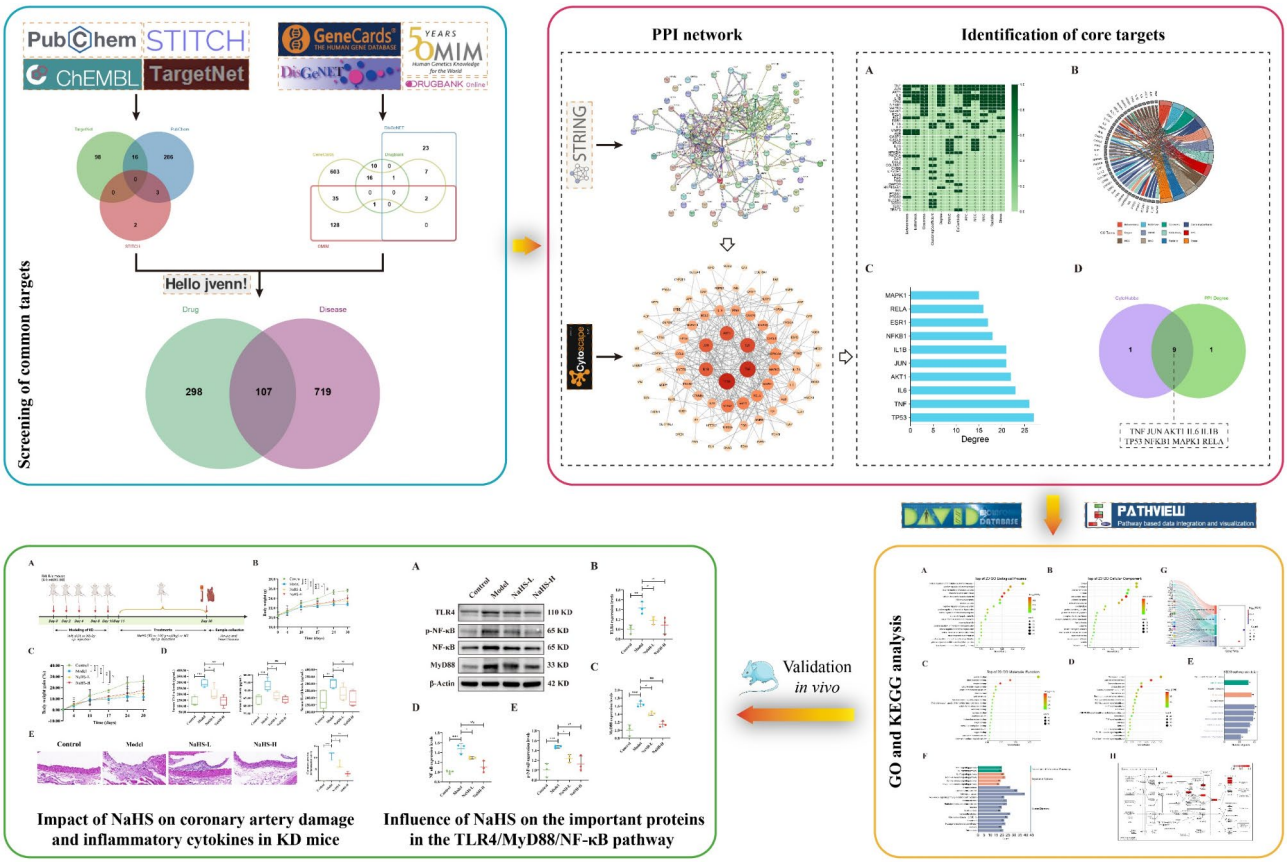

Fig. 1. Flowchart of the present study.

the top 10 targets were selected as the core targets of H_2S. Finally, a bioinformatics tool (http://www.bioinformatics.com.cn/) was used for visualizing the results.

GO and KEGG enrichment analysis

To predict the relationship between diseases and drug targets, the targets in PPI network underwent gene ontology (GO) and kyoto encyclopedia of genes and genomes (KEGG) enrichment analyses by the DAVID database (Version 2023q3, http://david.ncifcrf.gov)[31]. The identifier was set to "OFFICIAL_GENE_SYMBOL", the species limited to "Homo sapiens", and a threshold of FDR < 0.05 was applied. The results were exported and ranked in ascending order based on FDR values. The top 10 terms from GO analysis in biological process (BP), molecular function (MF), and cellular component (CC), as well as the top 10 pathways from the KEGG analysis, were visualized as histogram and bubble chart using the bioinformatics platform.

Mapping of core targets in critical signaling pathways

A comprehensive analysis was conducted based on previous documents and KEGG pathways enriched with core targets to identify the pivotal signaling pathway. Subsequently, the core targets were mapped onto the key pathway utilizing the PATHVIEW platform (https://pathview.uncc.edu/)[32]. This method provided a clear and intuitive visualization of the relationships between the essential target genes and the critical signaling pathways involved in the treatment of KD with H_2S.

Drugs and reagents

NaHS was procured from TargetMol Chemicals Inc. (Cat#T36503, Boston, MA, USA). Bovine serum albumin (BSA, purity > 98%) was obtained from Aladdin (Cat#B265993, Shanghai, China). TNFα enzyme-linked immunosorbent assay (ELISA) kit (Cat#SEA133Mu), IL-1β ELISA kit (Cat#SEA563Mu), and IL-6 ELISA kit (Cat#SEA079Mu) were purchased from Cloud-Clone Corp. (Wuhan, China). Primary antibodies for TLR4 (Cat#66350-1-Ig), NF-κB p65 (Cat#10745-1-AP), and MYD88 (Cat#67969-1-Ig) were supplied by Proteintech Group, Inc. (Wuhan, China). The p-NF-κB p65 (Thr254) antibody (Cat#GTX50097) was brought from GeneTex, Inc. (Irvine, CA, USA). Primary antibody against β-actin (Cat#52901-2) and the secondary antibodies HRP-conjugated goat anti-rabbit IgG (Cat#L3012) and goat anti-mouse IgG (Cat#L3032) were acquired by Signalway (Greenbelt, MD, USA).

Animal, KD model and treatment

A total of 32 male BALB/c mice (16–22 g) aged 4–6 weeks were obtained from Chengdu GemPharmatech Co., Ltd. (Chengdu, China). All animals were fed in an animal facility under controlled environmental conditions with humidity of 60–70% and a 12-h day/night cycle at 22 ± 2 °C. Throughout the study, the mice had free access to food and water. After one week of adaptive feeding, the mice were randomly assigned to four experimental groups (8 mice/group): control (Con), KD model (Model), low-dose NaHS (NaHS-L), and high-dose NaHS (NaHS-H). The KD model was established based on the protocol described by Qi et al.[33], where the mice in the Model, NaHS-L, and NaHS-H groups received intraperitoneal (i.p.) injections of a 10% BSA solution (once a day) on days 0, 2, 4, 8, and 10, while the Con group received normal saline (NS). Following the final injection for model induction, treatments were initiated. The Con and Model groups received NS, whereas the NaHS-L and NaHS-H groups were treated with NaHS at doses of 50 μmol/kg and 100 μmol/kg, respectively. Treatments were delivered via i.p. injection once daily for 20 consecutive days. The body weight of mice was measured on days 0, 4, 10, 17, 24, and 30 following the initiation of the model. At the end of the treatment period, mice were anesthetized via i.p. injection of pentobarbital sodium at a dose of 40 mg/kg, and heart tissues were harvested. Half of the heart samples was fixed in 4% paraformaldehyde (Cat# BL539A, Biosharp, Hefei, China) for histological analysis, while the other half was snap-frozen at −80 °C for subsequent western blot (WB) assays. Additionally, serum was collected and stored at −80 °C for the assessment of inflammatory cytokines. All animal procedures complied with the guidelines of the National Institutes of Health Guide for the Care and Use of Laboratory Animals (NIH publication No. 85 – 23, revised 1996), aiming to minimize animal pain, distress, and suffering caused by experiment. This project was approved by the Ethics Committee for Medical Research of Sichuan Provincial Women's and Children's Hospital. Furthermore, the study is reported in accordance with the ARRIVE guidelines (https://arriveguidelines.org).

Hematoxylin and Eosin (HE) staining

The heart tissue underwent HE staining to evaluate histopathological damage. Initially, the heart tissue fixed with 4% paraformaldehyde was rinsed and dehydrated, followed by paraffin embedding. The embedded tissue blocks were then sectioned transversely into 4 μm slices using a microtome (Leica, Shanghai, China) and dried at 60 °C overnight to ensure complete dehydration. After deparaffinization, the tissue sections were stained using a commercial HE constant dye kit (CAT#G1076; Servicebio, Shanghai, China) according to the supplier's instructions. Subsequently, the sections were cleared, mounted with neutral resin, and observed under an upright fluorescence microscope (Nikon, Tokyo, Japan) at magnifications of 10x and 40x to capture detailed images of the stained tissues. The histopathological assessment of coronary artery inflammation and the evaluation of lesion severity were conducted by an experienced coronary pathologist, who was blinded to the experimental group. A scoring system was employed to assess the acute inflammation, chronic inflammation, and fibroproliferation in the coronary arteries of KD. The scoring criteria for inflammation were as follows: 0 = no inflammation, 1 = sparse infiltration of inflammatory cells, 2 = scattered inflammatory cell presence, 3 = diffuse infiltration of inflammatory cells, and 4 = dense aggregation of inflammatory cells. To evaluate the degree of medial fibrosis in KD coronary arteries, the following scale was used: 0 = no medial fibrosis, 1 = fibrosis affecting less than 10% of the coronary artery intima, 2 = fibrosis involving 11–50% of the intima, 3 = fibrosis affecting 51–75% of the intima, and 4 = fibrosis involving more than 75% of the coronary artery intima. The four individual scores were combined to generate an overall severity score, referred to as the "vascular inflammation score"[34].

Measurement of inflammatory cytokines by ELISA

Levels of inflammatory cytokines, including interleukin (IL)−1β, IL-6, and tumor necrosis factor-α (TNF-α) in the serum of mice from each group were determined using ELISA kits. All assays were performed according to the manufacturer's protocols.

Western blot analysis

Total protein from fresh heart tissue was extracted by RIPA lysis buffer (CAT#P0013B; Beyotime, Shanghai, China) containing 1% PMSF (CAT#ST507-10 ml; Beyotime), 1% protease inhibitor (CAT# BR006; Signalway antibody), and 1% phosphatase inhibitor (CAT# K1007; APExBIO). Protein concentration of each sample was determined using an enhanced BCA protein assay kit (Beyotime). 20 μg protein per sample were then electrophoretically separated by 10% SDS-PAGE gels prepared with the PAGE gel preparation kit (CAT# PG112; chengdu baihe technology Co., Ltd., Chengdu, China) and transferred onto polyvinylidene fluoride (PVDF) membranes (CAT#1620177; Bio-Rad, CA, USA). The membranes were then blocked in 5% non-fat milk powder (CAT#1172GR100; BioFroxx, Guangdong, China) for 1 h. After blocking, the PVDF membranes underwent incubation with anti-TLR4 (1:2000), anti-MyD88 (1:5000), anti-NF-κB p65 (1:2000), anti-p-NF-κB p65 (Thr254) (1:500), and anti-β-actin (1:5000) primary antibodies overnight at 4 °C. Next day, the membranes were incubated with the HRP-conjugated goat anti-rabbit IgG (1:5000) or HRP-conjugated goat anti-mouse IgG (1:10000) secondary antibodies for 1 h at RT. The immunoblotted protein was imaged using an enhanced chemiluminescence (ECL) reagents kit (Bio-Rad) according to the manufacturer's instructions. The intensity of bands was analyzed via Evolution-Capt Edge software (Vilber, Collegien, France).

Statistical analysis

All statistical analyses were performed using SPSS 27.0 software, and the results are presented as mean ± standard deviation (SD). One-way analysis of variance (ANOVA) with the least-significant difference (LSD) or Games-Howell *post-hoc* test was applied to compare differences among three or more groups. A P-value lower than 0.05 was regarded as indicative of statistical significance.

Results

Identification of therapeutic targets for H_2S against KD

To systematically identify potential therapeutic targets for H_2S in KD, we utilized TargetNet, STITCH, and PubChem databases, identifying 114, 305, and 5 targets, respectively. After rigorous filtering, and removing duplicates, a total of 405 unique targets were obtained, representing the potential therapeutic scope of H_2S (Fig. 2A). To collect target genes for KD, we then queried the GeneCards, DisGeNET, OMIM, and DrugBank databases. This search returned 664 targets from GeneCards, 33 from DisGeNET, 166 from OMIM, and 28 from DrugBank. Following the removal of redundant entries, a total of 826 KD-related targets were retained (Fig. 2B). Finally, a Venn diagram analysis of these two target sets using the jVenn platform revealed an intersection of 107 overlapping targets. This subset of common targets was identified as potential therapeutic targets for H_2S in the treatment of KD and were selected for further analysis (Fig. 2C).

PPI network drawing

To elucidate the mechanisms underlying the therapeutic effects of H_2S on KD, we utilized the STRING database to perform a PPI topological network analysis for the 107 shared targets (Fig. 3A). This network comprises 107 nodes and 312 edges, with an average node degree of 5.83, an average local clustering coefficient of 0.448, and

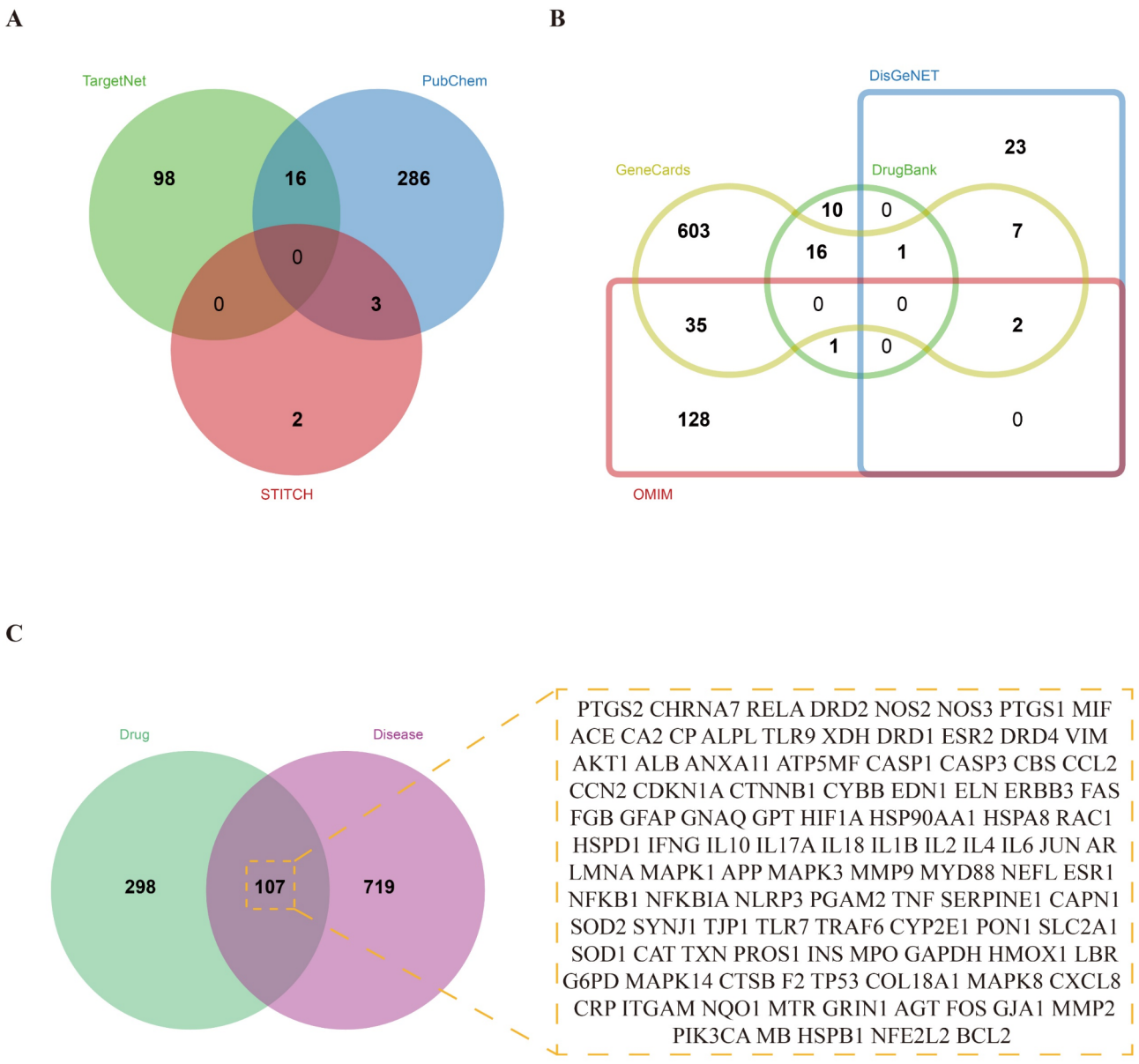

Fig. 2. Predicted targets of H_2S in KD. (**A**) Venn diagram depicting H_2S-related targets identified from three distinct databases. (**B**) Venn diagram illustrating KD-associated targets collected from four databases. (**C**) Overlapping targets potentially mediating H_2S anti-KD effects represented in a Venn diagram.

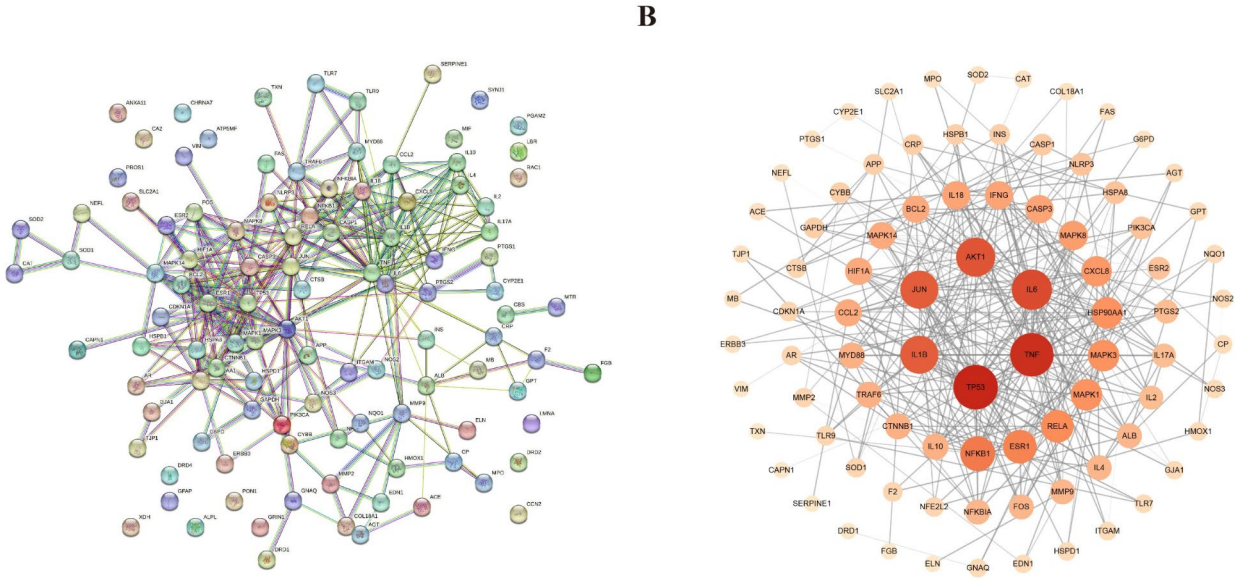

Fig. 3. PPI network analysis of shared targets in H_2S anti-KD action. (**A**) PPI network constructed by the STRING database. (**B**) PPI network visualized and analyzed in Cytoscape software. In the two networks, each "node" represents an interacting target protein, while each "edge" signifies the interactions between target proteins.

a PPI enrichment p-value of $< 1.0 \times 10^{-16}$. Subsequently, a refined PPI network consisting of 86 nodes and 311 edges, and featuring an increased average node degree of 7.23, was generated using Cytoscape 3.10.1 (Fig. 3B).

Identification of core therapeutic targets

To pinpoint hub genes for H_2S against KD, we employed 12 different CytoHubba algorithms (Degree, MCC, DMNC, MNC, EPC, Closeness, Betweenness, Clustering Coefficient, EcCentricity, Radiality, Stress, and BottleNeck) to extract the top 10 targets from the PPI network, culminating in a consolidated list of 40 unique genes. Figure 4A,B depict the relationships between these targets and the corresponding algorithms. Subsequently, the targets were prioritized based on the number of algorithms, and the top 10 genes were selected. They were then intersected with the leading 10 targets ranked by Degree in the PPI network (Fig. 4C), resulting in the identification of 9 key targets: TNF, IL6, JUN, AKT1, IL1B, TP53, NFKB1, MAPK1, and RELA (Fig. 4D).

The results of GO and KEGG enrichment analysis

To further investigate the molecular mechanisms of H_2S in treating KD, GO enrichment analysis was conducted on 86 targets identified from the PPI network constructed using Cytoscape 3.10.1, employing the DAVID database. A total of 306 significantly enriched GO terms (FDR < 0.05) were identified, including 246 BP, 26 CC, and 34 MF. The top 20 enrichment terms of BP, CC, and MF terms based on the lowest FDR values are visualized as bubble plots. The BP analysis results reveal that H_2S-targeted genes in KD are primarily associated with processes such as inflammatory response, positive regulation of IL-6 production, cellular response to TNF, cellular response to lipopolysaccharide, positive regulation of IL-1β production, and positive regulation of chemokine production (Fig. 5A). These targets are also notably enriched in CC, including cytosol, nucleus, extracellular region, and mitochondria (Fig. 5B). Moreover, H_2S targets are mainly involved in MF such as protein binding, enzyme binding, and cytokine activity (Fig. 5C).

To provide a comprehensive illustration of the potential mechanisms by which H_2S treats KD, KEGG pathway analysis was employed to predict the signaling pathways associated with the targets identified in the PPI network. A total of 162 pathways were identified through KEGG enrichment analysis (FDR < 0.05). Among these, the top 20 most significantly enriched pathways were selected based on the FDR value (Fig. 5D). Subsequently, a secondary classification of these 20 pathways revealed that the majority are involved in immune system regulation and the pathophysiology of human diseases such as infections and cardiovascular disorders (Fig. 5E). Further analysis, focusing on pathways associated with immune regulation, identified the IL-17, NOD-like receptor, Toll-like receptor, and C-type lectin receptor signaling pathways as key mechanisms through which H_2S may modulate immune responses relevant to KD pathogenesis (Fig. 5F). These pathways are known to play pivotal roles in inflammatory and immune processes implicated in KD. A Sankey diagram was constructed using a bioinformatics platform to visually display the data from these four critical pathways, providing a clear depiction of the interrelations between targets and pathways (Fig. 5G). Based on the findings from core target enrichment analysis and supporting literature, we speculate that H_2S may alleviate KD symptoms by modulating inflammatory responses through the Toll-like receptor signaling pathways. The distribution of key genes regulated by H_2S within the Toll-like receptor signaling pathway is presented in Fig. 5H. The above results imply that H_2S may exert its anti-KD effects through multiple mechanisms, with the Toll-like receptor signaling

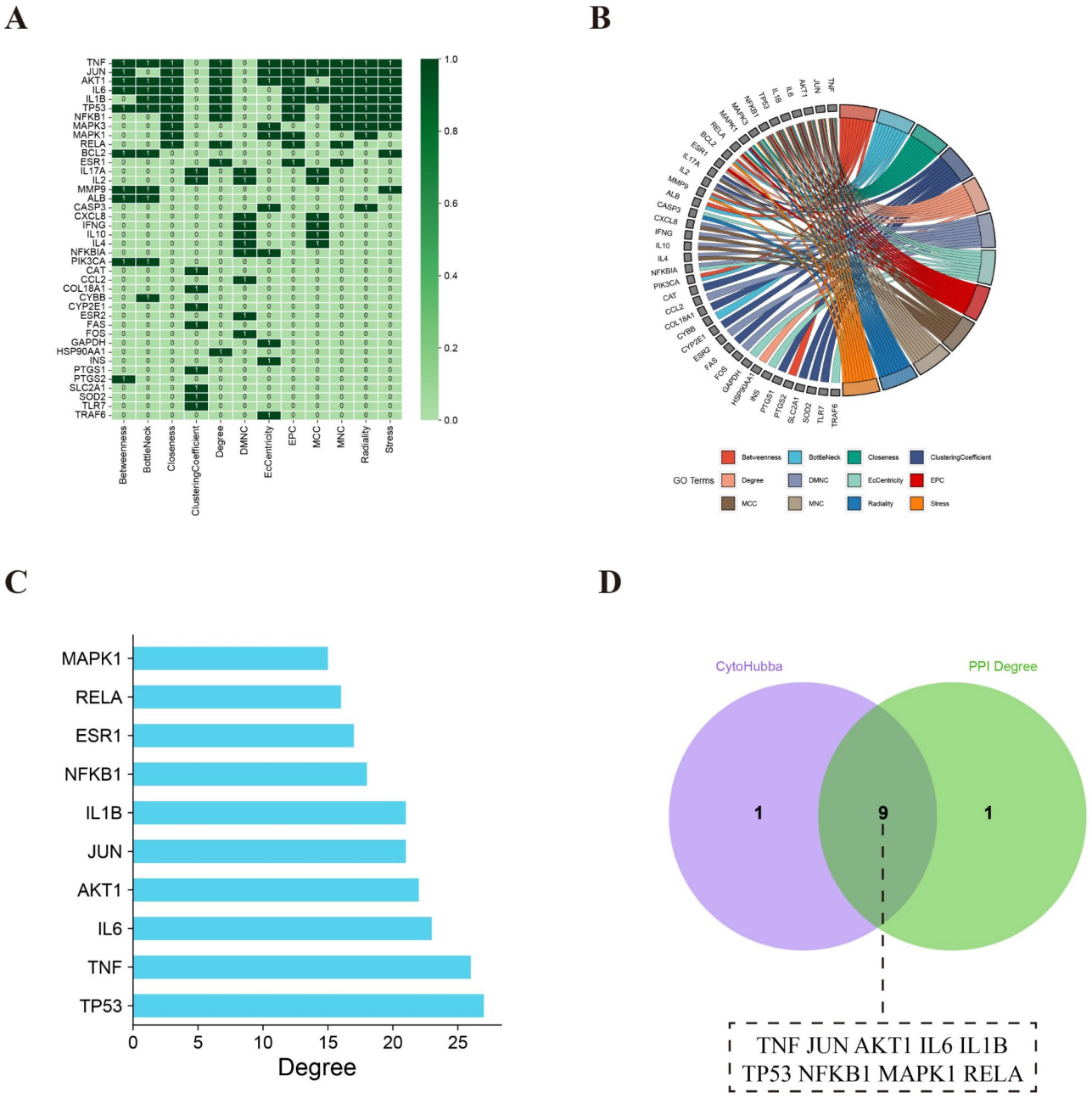

Fig. 4. Identification of core targets in H_2S anti-KD mechanism. (**A**) Heatmap showing associations between 12 CytoHubba algorithms and corresponding targets. (**B**) Chord diagram illustrating correlations between the top 10 targets and 12 CytoHubba algorithms. (**C**) Top 10 targets ranked by degree in the PPI network. (**D**) Venn diagram of intersected core targets derived from CytoHubba and PPI analyses.

pathway potentially playing a pivotal role. For in vivo experimental verification, we chose the TLR4/MyD88/NF-κB signaling pathway, which is closely related to the regulation of inflammatory pathogenesis.

H_2S attenuates coronary artery injury and inflammation in KD mice

To evaluate the effects of H_2S in the treatment of KD, we employed an exogenous H_2S donor, NaHS, in a KD mouse model induced by BSA. The experimental design is outlined in Fig. 6A. During the initial phase of the study, all groups exhibited a gradual increase in body weight, with no statistically significant differences compared to the control group ($P > 0.05$). However, significant changes in body weight were noted among the groups following the administration commenced at day 11. By the end of the 20-day treatment period, mice in all treated groups displayed significantly lower body weights compared to the control group, with statistical significance ($P < 0.001$). Notably, the NaHS-L and NaHS-H treatment groups demonstrated significantly higher body weights than the model group ($P < 0.05$ and $P < 0.01$) (Fig. 6B). Additionally, the percentage change in body weight post-treatment showed an increasing trend in all treated groups. The change in body weight of the

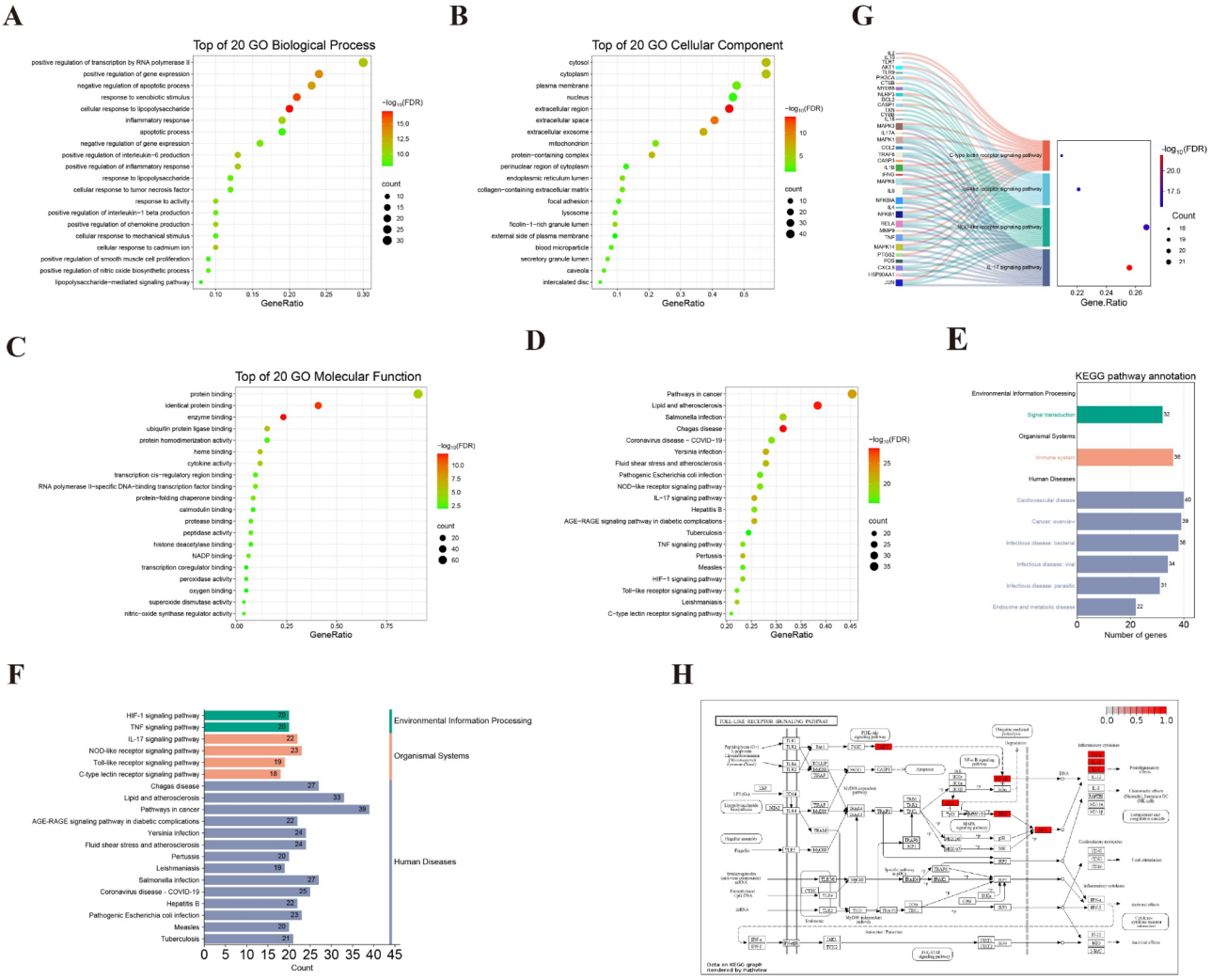

Fig. 5. GO and KEGG enrichment analysis of targets in the PPI network. (**A**) Bubble plot of enrichment in BP. (**B**) Bubble plot of enrichment in CC. (**C**) Bubble plot of enrichment in MF. (**D**) Bubble plot representing the top 20 pathways. (**E**) Bar chart showing secondary classification for the top 20 pathways. (**F**) Detailed bar chart of the primary classification of the top 20 pathways. (**G**) Sankey diagram linking the top 20 pathways to associated targets. (**H**) Distribution of core targets in the Toll-like receptor signaling pathway in KD[35–37].

NaHS-H group, in particular, showing a statistically significant higher over the model group by the conclusion of the treatment period (Fig. 6C). HE staining was performed on the coronary arteries of mice from each group to assess pathological changes. The histopathological analysis (Fig. 6E) revealed that the coronary artery intima of mice in the control group was characterized by a smooth and intact structure, with endothelial cells aligned uniformly and an absence of inflammatory cell infiltration in the surrounding regions. In contrast, the intima of the coronary artery in the model group displayed a roughened and disrupted morphology, marked by disorganized endothelial cell arrangement and significant structural disarray. Furthermore, the elastic membrane showed notable attenuation, accompanied by pronounced intimal thickening and considerable infiltration of inflammatory cells in the adjacent tissues. Encouragingly, exogenous supplementation of NaHS ameliorated these pathological alterations in the coronary arteries to different extents, with the high dose showing the most substantial improvements. Compared with the control group, the model mice exhibited significant coronary artery damage, as evidenced by a notably higher coronary inflammation score. Notably, both the NaHS-L and NaHS-H treatment groups demonstrated a statistically significant reduction in coronary inflammation scores compared to the model mice ($P<0.001$), with the NaHS-H group exhibiting the most pronounced attenuation. Moreover, the levels of inflammatory cytokines in mouse serum were measured using ELISA kits. The results indicated that a significant increase in TNF-α ($P<0.001$), IL-6 ($P<0.001$), and IL-1β ($P<0.01$) levels after BSA administration. Of note, NaHS treatment, especially at high dose, successfully reduced the levels of these inflammatory markers (Fig. 6D). Collectively, these data indicates that H_2S effectively mitigates growth retardation, promotes weight gain, alleviates the inflammatory response and attenuates coronary artery injury in BSA-induced KD mice, underscoring its potential as a candidate for therapeutic interventions in KD.

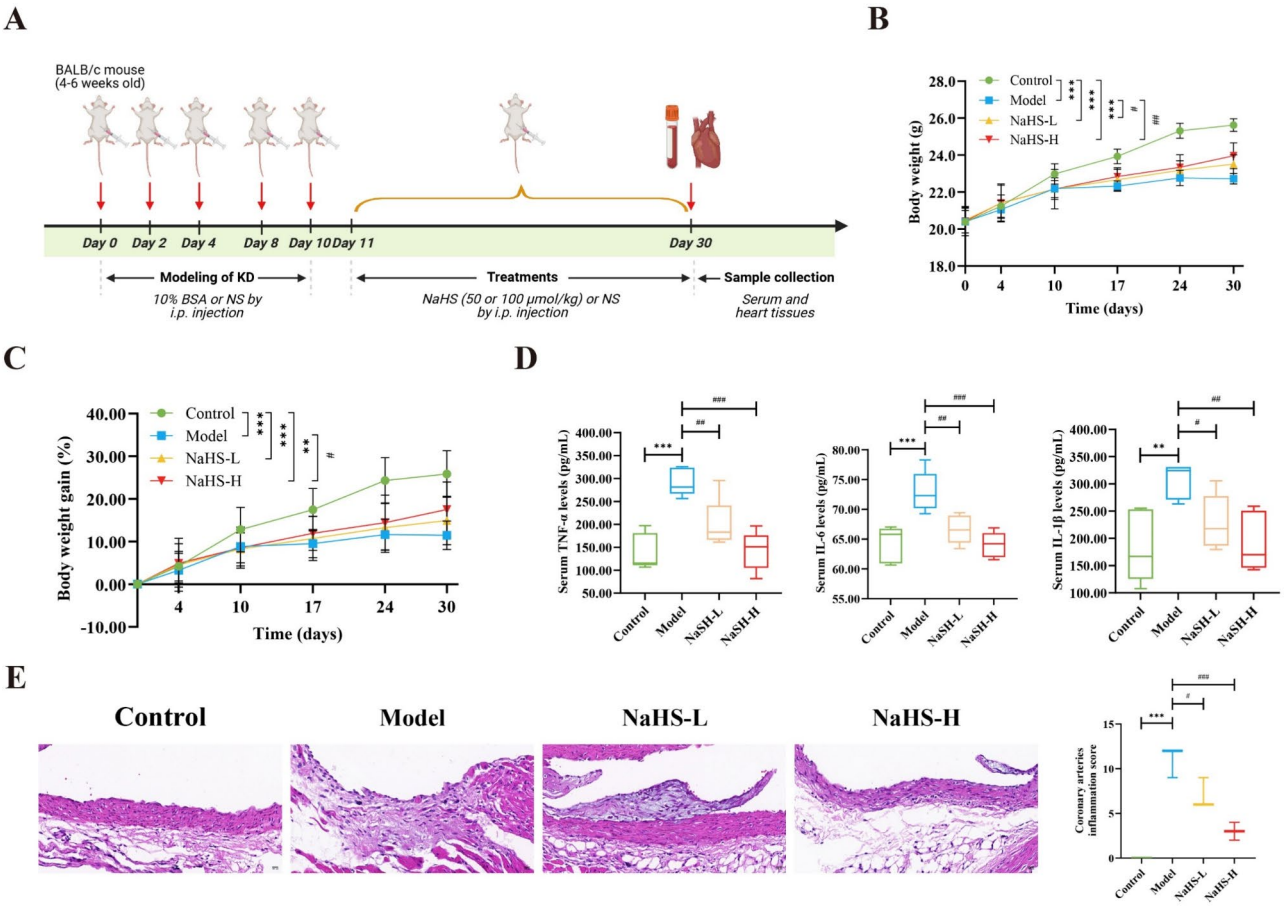

Fig. 6. Effects of exogenous H_2S on body weight, coronary artery damage and inflammatory cytokines in KD model mice. (**A**) Timeline of experimental design (created with BioRender.com). (**B**) Weight variation in mice over the experimental period. (**C**) Percentage of body weight gain across groups post-treatment. (**D**) Serum levels of TNF-α, IL-6, and IL-1β at the experiment's end. (**E**) HE staining results and inflammation score for coronary arteries at the experiment's end ($n = 3$). Data are expressed as mean ± SD. $^{**}P < 0.01$, $^{***}P < 0.001$ compared to the control group; $^{\#}P < 0.05$, $^{\#\#}P < 0.01$, $^{\#\#\#}P < 0.001$ compared to the model group. Data are presented as mean ± SD.

H_2S impedes TLR4/MyD88/NF-κB-mediated inflammatory signaling

We further validated the involvement of the TLR4/MyD88/NF-κB signaling pathway, as suggested by network pharmacology, in the anti-KD effects of H_2S by examining the expression of important proteins through WB analysis. The results demonstrated that the levels of TLR4, MyD88, NF-κB, and p-NF-κB were evidently upregulated in the heart tissue of mice in the model group ($P < 0.001$). Conversely, this augment was markedly inhibited by administration of NaHS in a dose-dependent manner (Fig. 7A–E). In brief, our findings confirm that one of the mechanisms by which exogenous H_2S attenuates KD is the suppression of inflammatory responses driven by TLR4/MyD88/NF-κB signaling.

Discussion

KD is a febrile vasculitis predominantly affecting small- to medium-sized arteries, especially the coronary arteries, which can lead to severe complications such as coronary artery aneurysms, thrombosis, and stenosis. In critical cases, KD may result in sudden death, representing the leading cause of acquired heart disease in children under five years of age[38]. However, the main treatment strategies, including IVIG and aspirin, are associated with limitations such as treatment resistance and bleeding risks[39,40]. Thus, the search for new therapeutic options is essential for improving the management of KD. H_2S, a third endogenous gaseous signaling molecule, plays a regulatory role in various physiological and pathological processes across multiple systems, including the cardiovascular system[41]. NaHS, a commonly used H_2S donor, has demonstrated protective effects against cardiovascular diseases such as atherosclerosis, heart failure, and myocardial ischemia-reperfusion injury through mechanisms involving anti-inflammatory, antioxidant, anti-apoptotic, and vascular protective actions[12]. Nonetheless, the potential role and underlying mechanisms of exogenous H_2S in KD-associated inflammation remain unexplored. This study aimed to investigate, for the first time, the anti-inflammatory effects of exogenous H_2S and the underlying mechanisms involved, using a combination of network pharmacology and experimental validation.

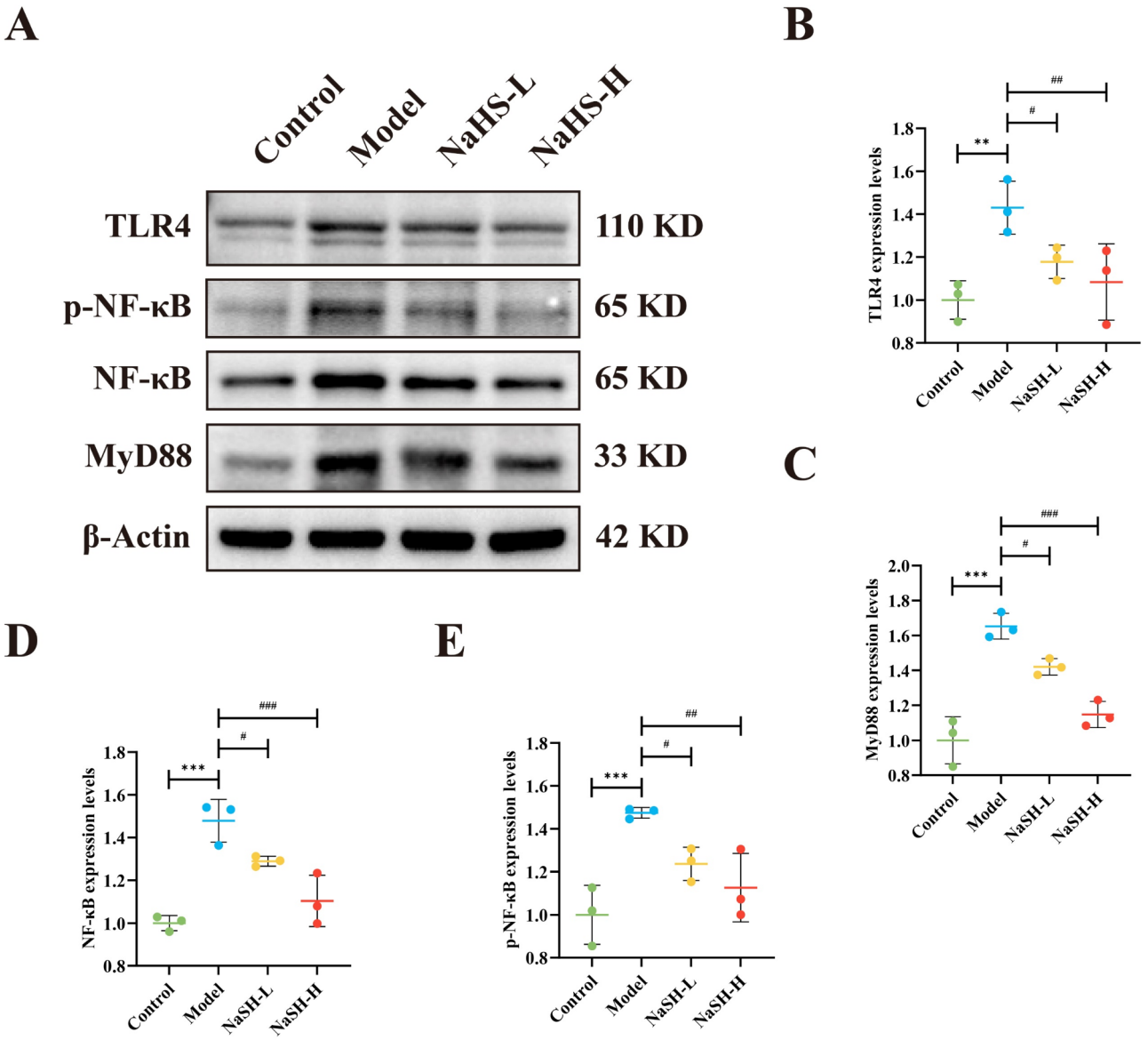

Fig. 7. Influence of exogenous H_2S on the TLR4/MyD88/NF-κB signaling pathway in KD model mice. (**A**) Representative western blot images of TLR4, MyD88, NF-κB, and p-NF-κB. (**B**–**E**) Quantitative analysis of expression levels for TLR4, MyD88, NF-κB, and p-NF-κB. Data are shown as mean ± SD ($n = 3$). $^{**}P < 0.01$, $^{***}P < 0.001$ compared to the control group; $^{\#}P < 0.05$, $^{\#\#}P < 0.01$, $^{\#\#\#}P < 0.001$ compared to the model group.

Network pharmacology is a systems biology-based approach that integrates methods from pharmacology, molecular biology, medicine, bioinformatics, computer science, and statistics. By constructing and analyzing drug-disease-target interaction networks, this approach predicts potential drug targets and mechanisms of action, providing insights into rational drug use and new drug discovery[42,43]. Based on it, we identified key targets such as TNF, IL6, JUN, AKT1, IL1B, TP53, NFKB1, MAPK1, and RELA, which are pivotal in the therapeutic effects of H_2S on KD. Notably, these targets are known to regulate inflammation, further underscoring their relevance to KD pathophysiology. To further elucidate the anti-inflammatory mechanisms of H_2S in KD, we conducted GO and KEGG enrichment analyses. Our findings suggest that H_2S may exert anti-KD effects by modulating key biological processes, including inflammatory response regulation and the production of pro-inflammatory mediators such as IL-6, TNF, IL-1β, and chemokines. Additionally, H_2S also influences several inflammation and immune-related pathways, including the Toll-like receptor (TLR), NOD-like receptor, and IL-17 signaling pathways. These results suggest that exogenous H_2S exerts its therapeutic effects through a multi-target, multi-pathway mechanism. The involvement of pathways associated with inflammation, immunity, and infection aligns with the established pathogenesis of KD[8].

Given the inherent limitations of network pharmacology, we further validated our findings through in vivo experiments. Based on previous reports by Qi et al.[33], who induced KD in BALB/c mice via intermittent i.p. injections of 10% BSA, we employed the same model for our study. Treatment with NaHS significantly

accelerated weight gain in KD mice, likely by alleviating inflammation and ameliorating symptoms, which in turn improved appetite and general physical condition. As KD primarily affects the coronary arteries, we evaluated coronary artery pathology using HE staining. The results indicated that exogenous H_2S supplementation reduced coronary intimal hyperplasia, structural disruption, and inflammatory cell infiltration. Furthermore, serum levels of IL-1β, TNF-α, and IL-6 were measured, and the data revealed a dose-dependent reduction in the contents of them following NaHS intervention. These pro-inflammatory cytokines, which play critical roles in inflammation, apoptosis, and cell survival, are implicated in autoimmune diseases and bacterial infections[44]. Research has shown that TNF-α[45], IL-6[46,47], and IL-1β[48] are elevated in the acute phase of KD, and blocking their release can significantly improve KD symptoms. Our findings suggest that exogenous H_2S effectively mitigates inflammatory responses and protects against vascular damage in KD. These observations are consistent with the anti-inflammatory effects reported for other therapeutic agents, such as liraglutide[49], Losartan[50], ginsenoside Rb1[33] and Xijiao Dihuang Tang[51], suggesting that H_2S may offer comparable benefits in KD management.

Given that TLR4, MyD88, NF-κB, and downstream factors, including TNF-α, IL-6, and IL-1β, serve as key targets within the KEGG-enriched Toll-like receptor pathway, which is known to mediate inflammatory responses and oxidative stress[52,53]. Therefore, H_2S is hypothesized to play a role in controlling KD by modulating inflammation through the TLR4/MyD88/NF-κB axis. TLRs are type I transmembrane pattern recognition

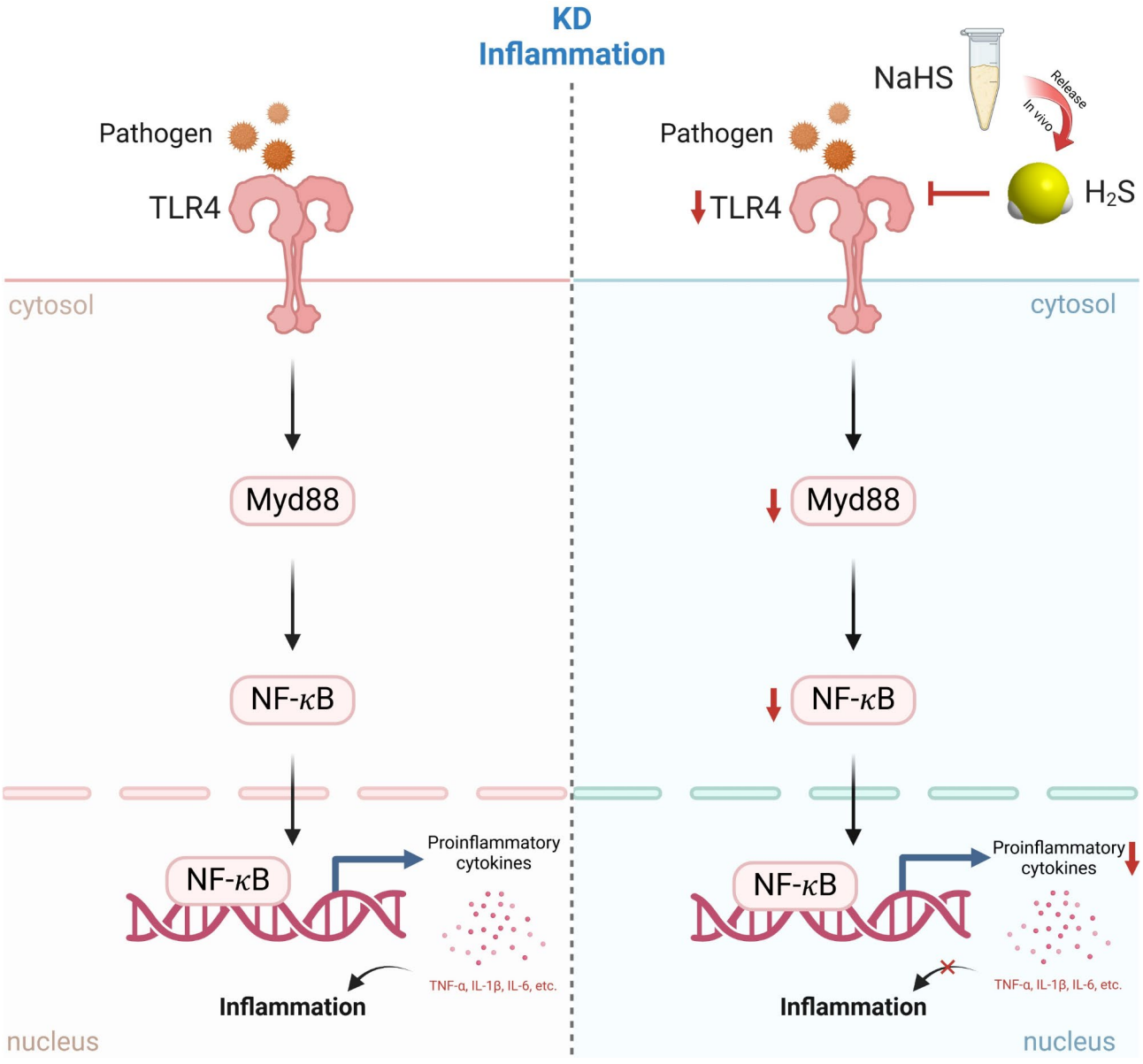

Fig. 8. Proposed molecular mechanism by which H_2S Inhibits inflammation in KD. In KD pathogenesis, multiple factors activate the TLR4/MyD88/NF-κB pathway, leading to systemic vascular inflammation and exacerbating coronary damage. H_2S suppresses the activation of the TLR4/MyD88/NF-κB pathway, reducing pro-inflammatory cytokine release, thereby mitigating inflammation and attenuating coronary lesions (created with BioRender.com).

receptors responsible for pathogen recognition and the initiation of innate immune responses by activating antigen-presenting cells and key cytokines, thus participating in both systemic inflammation and immunity. Among these, TLR4 is the most extensively studied receptor, while MyD88 is a key downstream adapter protein that plays a pivotal role in MyD88-dependent TLR signaling pathways. Upon activation, TLR4 induces MyD88-dependent NF-κB activation, leading to the expression of pro-inflammatory genes and promoting the release of IL-1β, TNF-α, etc., which contribute to the pathogenesis of various diseases[54]. Elevated levels of TLR4, MyD88, NF-κB, TNF-α, IL-6, and IL-1β has been observed in peripheral blood monocytes/macrophages from acute KD patients, suggesting that the hyperactivation of the TLR4/MyD88/NF-κB pathway contributes to immune dysfunction in KD[55–58]. Thus, targeting this pathway may restore immune homeostasis, reduce systemic inflammation, and improve KD outcomes. Furthermore, low doses of H_2S have been shown to inhibit inflammation by regulating the TLR4 pathway in various diseases[14,59–61]. Consequently, we examined the expression of important proteins in the TLR4/MyD88/NF-κB pathway in the heart tissue of KD mice using WB. The results revealed that the expression of TLR4, MyD88, NF-κB, and p-NF-κB were significantly elevated in the model group, while NaHS treatment markedly reduced their expression. These findings indicate that the protective effects of H_2S against KD-induced vasculitis are associated with inhibition of the TLR4/MyD88/NF-κB signaling.

Despite the promising results, this study has several limitations. First, the in vivo experiments were conducted primarily in a mouse model, and further studies, including in vitro experiments and clinical trials, are needed to confirm the findings. Second, although the importance of the TLR4/MyD88/NF-κB pathway was demonstrated, it remains unclear whether the anti-inflammatory effects of exogenous H_2S are exclusively dependent on this pathway. Future studies employing molecular biology techniques, such as overexpression or gene knockout models, are warranted to address this question. Additionally, we did not evaluate the efficacy of exogenous H_2S in comparison to or in combination with existing KD therapies, such as IVIG and aspirin. Investigating these aspects could help optimize treatment strategies. Future research will focus on these areas, facilitating a more comprehensive understanding for the therapeutic mechanisms of H_2S in KD and accelerating its potential clinical application.

Conclusions

In conclusion, this study introduced network pharmacology to preliminarily predict the core molecular targets and pathways through which H_2S might exert therapeutic effects in KD. Subsequently, the research demonstrated in a KD mouse model that exogenous H_2S remarkably alleviated coronary artery lesions, promoted weight recovery, and reduced the expression of key inflammatory cytokines. Of note, this is the first report to uncover that H_2S mitigates KD-related inflammation possibly by modulating the TLR4/MyD88/NF-κB signaling pathway (Fig. 8). These findings provide novel insights into H_2S-based therapeutic strategies and establish a promising new direction for the treatment of KD.

Data availability

Data will be made available from the corresponding author upon reasonable request.

Received: 23 November 2024; Accepted: 24 February 2025
Published online: 03 March 2025

References

1. Day-Lewis, M., Son, M. B. F. & Lo, M. S. Kawasaki disease: Contemporary perspectives. *Lancet Child Adolesc. Health* **8**, 781–792. https://doi.org/10.1016/S2352-4642(24)00169-X (2024).
2. Aggarwal, R. et al. Kawasaki disease and the environment: An enigmatic interplay. *Front. Immunol.* **14**, 1259094. https://doi.org/10.3389/fimmu.2023.1259094 (2023).
3. Kawasaki, T. Acute febrile mucocutaneous syndrome with lymphoid involvement with specific desquamation of the fingers and toes in children. *Arerugi* **16**, 178–222 (1967).
4. Kuo, H. C. Diagnosis, progress, and treatment update of Kawasaki disease. *Int. J. Mol. Sci.* **24**, 13948. https://doi.org/10.3390/ijms241813948 (2023).
5. Newburger, J. W. et al. A single intravenous infusion of gamma globulin as compared with four infusions in the treatment of acute Kawasaki syndrome. *N. Engl. J. Med.* **324**, 1633–1639. https://doi.org/10.1056/nejm199106063242305 (1991).
6. Newburger, J. W. et al. The treatment of Kawasaki syndrome with intravenous gamma globulin. *N. Engl. J. Med.* **315**, 341–347. https://doi.org/10.1056/nejm198608073150601 (1986).
7. Ferrara, G. et al. Anakinra for treatment-resistant Kawasaki disease: Evidence from a literature review. *Paediatr. Drugs* **22**, 645–652. https://doi.org/10.1007/s40272-020-00421-3 (2020).
8. Tang, B. et al. Adjuvant herbal therapy for targeting susceptibility genes to Kawasaki disease: An overview of epidemiology, pathogenesis, diagnosis and pharmacological treatment of Kawasaki disease. *Phytomedicine* **70**, 153208. https://doi.org/10.1016/j.phymed.2020.153208 (2020).
9. Chen, C. H. et al. Kawasaki disease with G6PD deficiency–report of one case and literature review. *J. Microbiol. Immunol. Infect.* **47**, 261–263. https://doi.org/10.1016/j.jmii.2012.05.002 (2014).
10. Tang, C., Li, X. & Du, J. Hydrogen sulfide as a new endogenous gaseous transmitter in the cardiovascular system. *Curr. Vasc. Pharmacol.* **4**, 17–22. https://doi.org/10.2174/157016106775203144 (2006).
11. Andrés, C. M. C. et al. Chemistry of hydrogen sulfide-pathological and physiological functions in mammalian cells. *Cells* **12**, 2684. https://doi.org/10.3390/cells12232684 (2023).
12. Kolluru, G. K. et al. Sulfide regulation of cardiovascular function in health and disease. *Nat. Rev. Cardiol.* **20**, 109–125. https://doi.org/10.1038/s41569-022-00741-6 (2023).
13. Song, Z. L. et al. Progress and perspective on hydrogen sulfide donors and their biomedical applications. *Med. Res. Rev.* **42**, 1930–1977. https://doi.org/10.1002/med.21913 (2022).
14. Xia, Y. et al. Hydrogen sulfide alleviates lipopolysaccharide-induced myocardial injury through TLR4-NLRP3 pathway. *Physiol. Res.* **72**, 15–25. https://doi.org/10.33549/physiolres.934928 (2023).

15. Liao, Y. et al. Exogenous H(2)S ameliorates high salt-induced hypertension by alleviating oxidative stress and inflammation in the paraventricular nucleus in Dahl S Rats. *Cardiovasc. Toxicol.* **22**, 477–491. https://doi.org/10.1007/s12012-022-09729-7 (2022).
16. Lu, H. Y. et al. Hydrogen sulfide attenuates aortic remodeling in aortic dissection associating with moderated inflammation and oxidative stress through a NO-dependent pathway. *Antioxidants (Basel)* **10**, 682. https://doi.org/10.3390/antiox10050682 (2021).
17. Hopkins, A. L. Network pharmacology: The next paradigm in drug discovery. *Nat. Chem. Biol.* **4**, 682–690. https://doi.org/10.1038/nchembio.118 (2008).
18. Yu, Z. et al. Network-based methods and their applications in drug discovery. *J. Chem. Inf. Model* **64**, 57–75. https://doi.org/10.1021/acs.jcim.3c01613 (2024).
19. Zdrazil, B. et al. The ChEMBL Database in 2023: A drug discovery platform spanning multiple bioactivity data types and time periods. *Nucleic Acids Res.* **52**, D1180–D1192. https://doi.org/10.1093/nar/gkad1004 (2024).
20. Wang, Y. et al. Integrated metabolomics and network pharmacology revealing the mechanism of arsenic-induced hepatotoxicity in mice. *Food Chem. Toxicol.* **178**, 113913. https://doi.org/10.1016/j.fct.2023.113913 (2023).
21. Yao, Z. J. et al. TargetNet: A web service for predicting potential drug-target interaction profiling via multi-target SAR models. *J. Comput. Aided Mol. Des.* **30**, 413–424. https://doi.org/10.1007/s10822-016-9915-2 (2016).
22. Szklarczyk, D. et al. STITCH 5: Augmenting protein-chemical interaction networks with tissue and affinity data. *Nucleic Acids Res.* **44**, D380-384. https://doi.org/10.1093/nar/gkv1277 (2016).
23. Kim, S. et al. PubChem 2023 update. *Nucleic Acids Res.* **51**, D1373–D1380. https://doi.org/10.1093/nar/gkac956 (2023).
24. Stelzer, G. et al. The GeneCards suite: From gene data mining to disease genome sequence analyses. *Curr. Protoc. Bioinform.* **54**, 1–30. https://doi.org/10.1002/cpbi.5 (2016).
25. Piñero, J. et al. The DisGeNET knowledge platform for disease genomics: 2019 update. *Nucleic Acids Res.* **48**, D845–D855. https://doi.org/10.1093/nar/gkz1021 (2020).
26. Amberger, J. S. et al. OMIM.org: Online Mendelian inheritance in Man (OMIM®), an online catalog of human genes and genetic disorders. *Nucleic Acids Res.* **43**, D789-798. https://doi.org/10.1093/nar/gku1205 (2015).
27. Knox, C. et al. DrugBank 6.0: The DrugBank knowledgebase for 2024. *Nucleic Acids Res.* **52**, D1265–D1275. https://doi.org/10.1093/nar/gkad976 (2024).
28. Bardou, P. et al. jvenn: An interactive Venn diagram viewer. *BMC Bioinform.* **15**, 293. https://doi.org/10.1186/1471-2105-15-293 (2014).
29. Szklarczyk, D. et al. The STRING database in 2023: Protein-protein association networks and functional enrichment analyses for any sequenced genome of interest. *Nucleic Acids Res.* **51**, D638–D646. https://doi.org/10.1093/nar/gkac1000 (2023).
30. Liu, C. et al. Integrating network pharmacology, transcriptomics, and molecular simulation to reveal the mechanism of tert-butylhydroquinone for treating diabetic retinopathy. *Eur. J. Pharmacol.* **931**, 175215. https://doi.org/10.1016/j.ejphar.2022.175215 (2022).
31. Sherman, B. T. et al. DAVID: A web server for functional enrichment analysis and functional annotation of gene lists (2021 update). *Nucleic Acids Res.* **50**, W216–W221. https://doi.org/10.1016/10.1093/nar/gkac194 (2022).
32. Luo, W. et al. Pathview Web: User friendly pathway visualization and data integration. *Nucleic Acids Res.* **45**, W501–W508. https://doi.org/10.1093/nar/gkx372 (2017).
33. Qi, S. H. et al. Value of ginsenoside Rb1 in alleviating coronary artery lesion in a mouse model of Kawasaki disease. *Zhongguo Dang Dai Er Ke Za Zhi* **22**, 1034–1040. https://doi.org/10.7499/j.issn.1008-8830.2003147 (2020).
34. Lombardi Pereira, A. P. et al. Long-term cardiovascular inflammation and fibrosis in a murine model of vasculitis induced by Lactobacillus casei cell wall extract. *Front. Immunol.* **15**, 1411979. https://doi.org/10.3389/fimmu.2024.1411979 (2024).
35. Kanehisa, M. & Goto, S. KEGG: Kyoto encyclopedia of genes and genomes. *Nucleic Acids Res.* **28**, 27–30. https://doi.org/10.1093/nar/28.1.27 (2000).
36. Kanehisa, M. Toward understanding the origin and evolution of cellular organisms. *Protein Sci.* **28**, 1947–1951. https://doi.org/10.1002/pro.3715 (2019).
37. Kanehisa, M. et al. KEGG for taxonomy-based analysis of pathways and genomes. *Nucleic Acids Res.* **51**, D587–D592. https://doi.org/10.1093/nar/gkac963 (2023).
38. Agarwal, S. & Agrawal, D. K. Kawasaki disease: etiopathogenesis and novel treatment strategies. *Expert. Rev. Clin. Immunol.* **13**, 247–258. https://doi.org/10.1080/1744666X.2017.1232165 (2017).
39. Kibata, T. et al. Coronary artery lesions and the increasing incidence of Kawasaki disease resistant to initial immunoglobulin. *Int. J. Cardiol.* **214**, 209–215. https://doi.org/10.1016/j.ijcard.2016.03.017 (2016).
40. Zheng, X. et al. Efficacy between low and high dose aspirin for the initial treatment of Kawasaki disease: Current evidence based on a meta-analysis. *PLoS One* **14**, e0217274. https://doi.org/10.1371/journal.pone.0217274 (2019).
41. Cirino, G., Szabo, C. & Papapetropoulos, A. Physiological roles of hydrogen sulfide in mammalian cells, tissues, and organs. *Physiol. Rev.* **103**, 31–276. https://doi.org/10.1152/physrev.00028.2021 (2023).
42. Wu, Z. et al. Network-based methods for prediction of drug-target interactions. *Front. Pharmacol.* **9**, 1134. https://doi.org/10.3389/fphar.2018.01134 (2018).
43. Zhao, L. et al. Network pharmacology, a promising approach to reveal the pharmacology mechanism of Chinese medicine formula. *J. Ethnopharmacol.* **309**, 116306. https://doi.org/10.1016/j.jep.2023.116306 (2023).
44. Kany, S., Vollrath, J. T. & Relja, B. Cytokines in inflammatory disease. *Int. J. Mol. Sci.* **20**, 6008. https://doi.org/10.3390/ijms20236008 (2019).
45. Chen, J. et al. Current knowledge of TNF-α monoclonal antibody infliximab in treating Kawasaki disease: A comprehensive review. *Front. Immunol.* **14**, 1237670. https://doi.org/10.3389/fimmu.2023.1237670 (2023).
46. Fuster, J. J. & Walsh, K. The good, the bad, and the ugly of interleukin-6 signaling. *Embo J.* **33**, 1425–1427. https://doi.org/10.15252/embj.201488856 (2014).
47. Scheller, J. et al. The pro- and anti-inflammatory properties of the cytokine interleukin-6. *Biochim. Biophys. Acta* **1813**, 878–888. https://doi.org/10.1016/j.bbamcr.2011.01.034 (2011).
48. Hoang, L. T. et al. Global gene expression profiling identifies new therapeutic targets in acute Kawasaki disease. *Genome Med.* **6**, 541. https://doi.org/10.1186/s13073-014-0102-6 (2014).
49. Ding, Y. et al. The protective roles of liraglutide on Kawasaki disease via AMPK/mTOR/NF-κB pathway. *Int. Immunopharmacol.* **117**, 110028. https://doi.org/10.1016/j.intimp.2023.110028 (2023).
50. Suganuma, E. et al. Losartan attenuates the coronary perivasculitis through its local and systemic anti-inflammatory properties in a murine model of Kawasaki disease. *Pediatr. Res.* **81**, 593–600. https://doi.org/10.1038/pr.2016.266 (2017).
51. Zhang, J. et al. Protective roles of Xijiao Dihuang tang on coronary artery injury in Kawasaki disease. *Cardiovasc. Drugs Ther.* **37**, 257–270. https://doi.org/10.1007/s10557-021-07277-w (2023).
52. Zhang, Q. et al. Signaling pathways and targeted therapy for myocardial infarction. *Signal Transduct. Target Ther.* **7**, 78. https://doi.org/10.1038/s41392-022-00925-z (2022).
53. Zhou, J. et al. Inappropriate activation of TLR4/NF-κB is a cause of heart failure. *CVIA* **7**, 73–89. https://doi.org/10.15212/CVIA.2022.0020 (2022).
54. Fitzgerald, K. A. & Kagan, J. C. Toll-like receptors and the control of immunity. *Cell* **180**, 1044–1066. https://doi.org/10.1016/j.cell.2020.02.041 (2020).
55. Wang, G. B. et al. Changes and significance for regulatory factors for signal pathways of Toll-like receptors in immunological pathogenesis of Kawasaki disease. *Zhonghua Er Ke Za Zhi* **46**, 49–54 (2008).

56. Wang, G. B. et al. The role of activation of toll-like receptors in immunological pathogenesis of Kawasaki disease. *Zhonghua Er Ke Za Zhi* **44**, 333–336 (2006).
57. Furukawa, S., Matsubara, T. & Ichiyama, T. Regulation of proinflammatory cytokine cascade in Kawasaki disease. *Nihon Rinsho* **66**, 258–264 (2008).
58. Qi, X. L. et al. 1,25-Dihydroxyvitamin D3 regulates T lymphocyte proliferation through activation of P53 and inhibition of ERK1/2 signaling pathway in children with Kawasaki disease. *Eur. Rev. Med. Pharmacol. Sci.* **21**, 3714–3722 (2017).
59. Chen, Y. et al. Hydrogen sulfide attenuates LPS-induced acute kidney injury by inhibiting inflammation and oxidative stress. *Oxid. Med. Cell Longev.* **2018**, 6717212. https://doi.org/10.1155/2018/6717212 (2018).
60. Chen, Y. H. et al. Hydrogen sulfide attenuated sepsis-induced myocardial dysfunction through TLR4 pathway and endoplasmic reticulum stress. *Front. Physiol.* **12**, 653601. https://doi.org/10.3389/fphys.2021.653601 (2021).
61. Zhang, G. Y. et al. Hydrogen sulfide alleviates lipopolysaccharide-induced diaphragm dysfunction in rats by reducing apoptosis and inflammation through ROS/MAPK and TLR4/NF-κB signaling pathways. *Oxid. Med. Cell Longev.* **2018**, 9647809. https://doi.org/10.1155/2018/9647809 (2018).

Acknowledgements

We sincerely appreciate the developers of the databases and software utilized in this study for their invaluable contributions. We also extend our heartfelt gratitude to Figdraw (www.Figdraw.com) for their essential support in creating schematic diagrams, which significantly enhanced the efficiency and impact of our research.

Author contributions

LY: Writing - Original Draft, Software, Validation, Investigation, Formal analysis, Data curation. QWL: Validation, Investigation, Software, Formal analysis. XHR: Validation, Investigation, Visualization. XX: Supervision, Visualization. PHW: Conceptualization, Methodology, Resources, Data curation, Writing - Review & Editing, Supervision, Project administration, Funding acquisition.

Funding

This work received the funding from the Scientific and Technological Innovation Foundation of Sichuan Provincial Maternity and Child Health Care Hospital (CXZD2022-01).

Declarations

Competing interests

The authors declare no competing interests.

Additional information

Correspondence and requests for materials should be addressed to P.W.

Reprints and permissions information is available at www.nature.com/reprints.

Publisher's note Springer Nature remains neutral with regard to jurisdictional claims in published maps and institutional affiliations.

Open Access This article is licensed under a Creative Commons Attribution-NonCommercial-NoDerivatives 4.0 International License, which permits any non-commercial use, sharing, distribution and reproduction in any medium or format, as long as you give appropriate credit to the original author(s) and the source, provide a link to the Creative Commons licence, and indicate if you modified the licensed material. You do not have permission under this licence to share adapted material derived from this article or parts of it. The images or other third party material in this article are included in the article's Creative Commons licence, unless indicated otherwise in a credit line to the material. If material is not included in the article's Creative Commons licence and your intended use is not permitted by statutory regulation or exceeds the permitted use, you will need to obtain permission directly from the copyright holder. To view a copy of this licence, visit http://creativecommons.org/licenses/by-nc-nd/4.0/.

© The Author(s) 2025